

Contents list available at **IJND**
International Journal of Nano Dimension

Journal homepage: www.IJND.ir

Anatase TiO₂ and mixed M-Anatase TiO₂ (M = CeO₂ or ZrO₂) nano powder: Synthesis and characterization

ABSTRACT

O. Zuas*
H. Budiman
N. Hamim

*Research Centre for Chemistry,
Indonesian Institute of Sciences
(RCChem-LIPI) Kawasan
PUSPIPTEK Serpong, 15314,
Tangerang, Banten, Indonesia.*

Received 07 June 2012

Accepted 06 September 2012

Pure Anatase Titania (TiO₂), mixed 1.0 wt.% Cerium-Anatase Titania (1.0 wt.% CeO₂-TiO₂), and mixed 1.0 wt.% Zirconia-Anatase Titania (1.0 wt.% ZrO₂-TiO₂) nano powders were synthesized by co-precipitation method and characterized using X-ray diffraction (XRD), Brunauer-Emmett-Teller (BET) surface area analysis, UV-Vis diffuse reflectance spectroscopy (DRS), and transmission electron microscope (TEM) technique. The characterization results indicated that the crystal powders of the synthesized TiO₂-based material were estimated nanometer in size and predominantly in the form of anatase with good crystalline nature. The grain sizes of the powders were observed in the range of 7.65 – 12.56 nm. The presence of the CeO₂ and ZrO₂ in TiO₂ matrix has shifted the adsorption edge to higher wavelength region (red shift) in addition to increase the BET specific surface area. This study indicated that the CeO₂ and ZrO₂ demonstrated a beneficial effect on the structural and optical properties of TiO₂.

Keywords: *Anatase; Titania; Ceria; Zirconia; Co-precipitation; Nano powder.*

INTRODUCTION

In our daily life, titanium dioxide (TiO₂) is one of the most important transition metal semiconductor materials that has been widely used as material in fuel cell, solar energy conversion, photocatalysts, white pigment in paints and paper, bone implant material, UV absorber in sunscreen cream and other cosmetic products, and additive in food products [1-4]. The broad application of the TiO₂ is due to its outstanding properties such as harmless, relative inexpensive, chemically stable, and environmentally friendly [5-7]. In the area of heterogeneous photocatalysis, TiO₂ is particularly employed to enhance the efficiency of the environmental remediation process involving reduction-oxidation reaction.

* Corresponding author:

Oman Zuas
Research Centre for Chemistry,
Indonesian Institute of Sciences
(RCChem-LIPI), Kawasan
PUSPIPTEK Serpong, 15314,
Tangerang, Banten, Indonesia.
Tel +62 217560929
Fax +62 217560549
Email oman.zuas@lipi.go.id

Concerning to the efficiency enhancement on the photocatalytic applications, intrinsic properties of the TiO₂ such crystalline phase, surface area, and band gap play an important role. Anatase and rutile are the two common crystalline phase of TiO₂ in which the anatase type exhibits higher overall photocatalytic activity than the rutile type [8, 9]. TiO₂ with specific surface area is also essential because it could increase in specific surface active site for chemical reaction and photon adsorption [10]. In addition, TiO₂ is well known semiconductor with relatively high band gap (3.2 eV) which can only be excited by higher energy UV at a wavelength shorter than 387 nm [11]. Modification the TiO₂ having lower band gap is advantage which can further promote the TiO₂ to adsorb light at a higher wavelength region (>387 nm) [12].

In this report, we describe a scientific work on synthesis of pure anatase TiO₂, mixed 1.0 wt. % CeO₂-anatase TiO₂ and 1.0 wt. % ZrO₂-anatase TiO₂ by the co-precipitation method. The intrinsic properties of the synthesized TiO₂-based nanomaterial were characterized by XRD, BET specific surface area, UV-Vis DRS and TEM techniques.

EXPERIMENTAL

Materials

All chemicals used were analytic grade and used as received without further purification. Titanium tetrachloride (TiCl₄), cerium (III) nitrate hexahydrate (CeNO₃.6H₂O), zirconium (II) chloride (ZrCl₂), aqueous ammonia (NH₄OH, 25%), N-Cetyl-N,N,N-trimethylammonium bromide (CTAB), sodium hydroxide (NaOH) and purified water (Millipore Corp., 17.5 MΩ·cm).

Methods

- **Synthesis of nanostructured materials**

Nanostructured powder of pure titania (denoted as P-TiO₂), mixed ceria-titania (denoted as 1.0 wt.% Ce-Ti oxides), and mixed zirconia-titania (denotes as 1.0 wt.% Zr-Ti oxides) were synthesized by a co-precipitation. In a typical experiment: desired amount of CTAB was firstly dissolved in purified water (Solution-A) and stored in the freezer to keep its temperature close to

freezing point for further use. A concentrated TiCl₄ solution was slowly dropped into Solution-A under vigorous stirring (Solution-B). The molar ratio of CTAB:Ti in Solution-B was 0.2. An appropriate amount of CeNO₃.6H₂O or ZrCl₂ with required percentage (1.0 wt.%) was added into Solution-B under stirring for 5 min (Solution-C). Subsequently, an aqueous NH₄OH solution was added dropwise (5 ml/min) into Solution-C under stirring until the pH value of the solution was 10. The solution was then aged at 55-60°C for 6 h. A solid after aging treatment was separated from the solution by centrifugation at 8000 rpm for 10 min, washed with distilled water until no Cl⁻ ions in the filtrate could be detected. The wet solid precursors were dried at 100°C for 12 h to produce dry solid precursors followed by calcining at 450°C in open air using in a tube box muffle furnace with programmed temperature mode for 4 h to produce 1.0 wt.% Ce-Ti oxides or 1.0 wt.% Zr-Ti oxides. Pure TiO₂ was also synthesized with same procedure without CeNO₃.6H₂O or ZrCl₂.

- **Characterization of synthesized materials**

The X-ray diffraction (XRD) spectra were obtained at room temperature on a Rigaku X-ray diffraction with Cu (k = 1.5406 Å) irradiation and scanned over a 2θ range of 20-70° at a scanning speed of 1.2°/min. The diffuse reflectance spectra (DRS) were recorded on a Shimadzu UV2450 spectrophotometer under ambient temperature and BaSO₄ was used as a reference. The specific surface area (S_{BET}) was calculated from a multipoint BET (Brunauer-Emmett-Teller) analysis of nitrogen adsorption isotherm using a Micrometrics ASAP 2010 surface area analyzer. The surface morphological of the sample was observed from electron micrographs obtained with a Tecnai G2 F20 transmission electron microscopy (TEM) operated at 200 kV.

RESULTS AND DISCUSSION

X-ray diffraction

XRD diffraction profiles of the synthesized nanostructured powders are shown in Figure 1. From the XRD profile of P-TiO₂ (Figure 1a), it can be seen that P-TiO₂ sample gave well-established diffraction peaks at (2θ) at about 25°,

38°, 48°, 54°, 55°, 63°, and 69°, which are ascribed to the (101), (004), (200), (105), (211), (204), and (116) reflection planes, respectively, corresponds to the pure anatase phase according to JCPDS Card No. 21-1272. While brookite- and rutile-related peaks are absence, indicating that calcining temperature employed under this study was suitable for the formation of anatase phase. A similar characteristic of the XRD profile was found in both 1.0 wt.% Ce-Ti oxides (Figure 1b) and 1.0 wt.% Zr-Ti oxide (Figure 1c) nanostructured samples. In addition, neither CeO₂ nor ZrO₂ characteristic peaks can be observed. Characteristically, no XRD diffraction peaks of the metal impurities in a TiO₂-metal oxide mixture could be explained as a result of low metal content added during the synthesis process or the metal has been well-dispersed on TiO₂ particles as a small cluster [13].

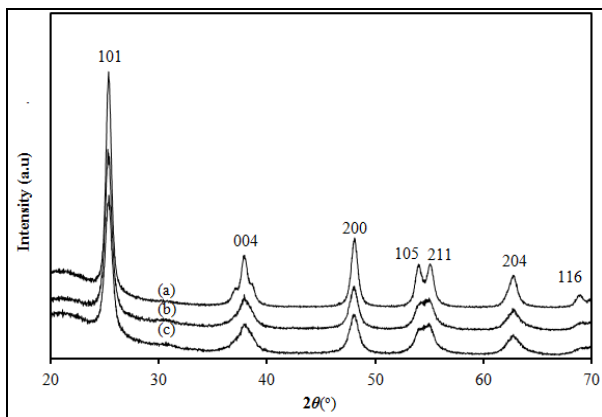


Fig. 1. XRD profiles of the synthesized nano powder: (a) P-TiO₂, (b) 1.0 wt.% Ce-Ti oxide, and (c) 1.0 wt.% Zr-Ti oxide.

The average crystallite size of the synthesized samples were calculated from the full-width at half-maximum (FWHM) of anatase [101] reflection using Scherrer's formula [14, 15]: $D = 0.9 \lambda / \beta \cos \theta$, where D is the crystallite size, λ is the wavelength of the X-ray diffraction, β is the FWHM, θ is the angle of diffraction. The results of crystallite size calculation for each synthesized nano powder are listed in Table 1. As can be seen from Table 1, the crystallite size of synthesized sample containing ZrO₂ and CeO₂ are smaller than P-TiO₂ follows the order: 1.0 wt.% Zr-Ti oxide < 1.0 wt.% Ce-Ti oxide < P-TiO₂. Decreasing the crystallite size of both metal oxide-containing samples might be ascribed as a

broadening effect of the CeO₂ and ZrO₂ resulting in a wider of the anatase [101] reflection peak (Figure 2). In a word, broadening the width of the [101] reflection peak led to decrease the calculated crystallite size correspondingly. In addition, unshifted the peak [101] reflection of anatase crystal of the ZrO₂ and CeO₂-containing sample relative to P-TiO₂ (Figure 2) indicated that the Zr and Ce did not perturb the TiO₂ lattices. Owing to the higher ionic radii of both Zr⁴⁺ (~0.84Å) and Ce⁴⁺ (~0.97 Å) would be energetically inauspicious for substituting Ti⁴⁺ (~0.68Å) position. In other words, the Zr and Ce are probably located on the TiO₂ surface, in the form of cluster, instead of entering the TiO₂ crystal lattice. A similar finding has been previously reported regarding the effect of ZnO on the characteristic of TiO₂ [15-17].

Table 1. Intrinsic properties of the synthesized nano powder

Sample	Crystallite size (nm)	Band gap (eV)	Adsorption edges (nm)	BET Surface area (m ² /g)
P-TiO ₂	12.3	3.32	372	71.02
1.0 wt.% Ce-Ti oxide	9.4	3.26	379	98.15
1.0 wt.% Zr-Ti oxide,	8.9	3.20	386	116.35

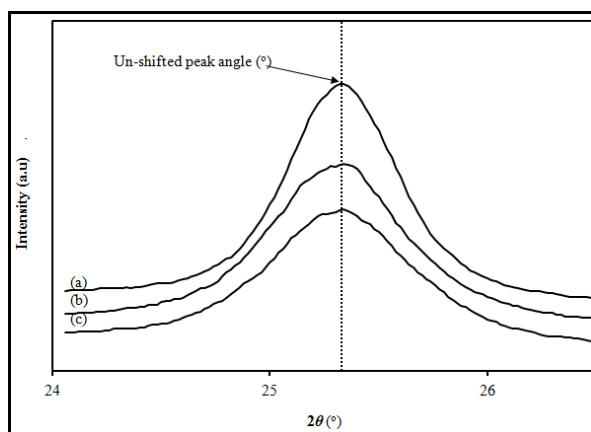


Fig. 2. Peak [101] reflection plane of : (a) P-TiO₂, (b) 1.0 wt.% Ce-Ti oxides, and (c) 1.0 wt.% Zr-Ti oxides

BET surface area

The BET surface areas of synthesized samples are listed in Table 1 from which it is evident that the presence of CeO₂ and ZrO₂ exhibits a significant change in the surface area of the synthesized nano powder. It is clear that both 1.0 wt.% Ce-Ti oxide and 1.0 wt.% Zr-Ti oxide have specific surface area that far exceeds the P-TiO₂ nano powder. The synthesized 1.0 wt.% Zr-Ti oxide nano powder sample was found to have the largest specific surface increasing by about 38.96%, while specific surface area of 1.0 wt.% Ce-Ti oxide nano powder increased by about 27.64% relative to P-TiO₂. Considering the BET surface area calculations that resulted from this experiment, the presence CeO₂ and ZrO₂ into TiO₂ matrix would be of paramount importance for TiO₂ as a solid reactant to maximize the rate of reaction. Generally speaking, the larger the surface area provides the advantage for more reaction take place at phase interface lead to better reaction process efficiency [18]. Similar observation regarding the effect of metal oxide addition such as copper and zinc on the specific surface area of TiO₂ has been reported by previous researchers [19, 20].

Diffuse reflectance spectroscopy

Adsorption light capacity of TiO₂-based materials is very important because it would affect to the process efficiency of a photoreaction, as the more extent the light adsorption spectrum; the more improve the light efficiency utilization. The light absorbance characteristics of the synthesized nano powder were investigated in the UV-visible range. The measured reflectance spectra obtained were transformed into Kubelka-Munk function, $(F(R)) = (1 - R)^2 / 2R$, where R is the reflectance value of the sample. The estimated band gap energy (E_g) of the photocatalyst samples was generated by substituting the adsorption edge (λ , nm) values, which was generated by plotting between the K-M function against wavelength as shown in Figure 3 for instance, into the formula: E_g (eV) = $1236 / \lambda(\text{nm})$ [21]. Basis of this calculation, the E_g for the synthesized nanostructured samples are listed in Table 1. As can be seen from Table 1, the adsorption edges of the 1.0 wt.% Ce-Ti oxides and 1.0 wt.% Zr-Ti oxide nano powder significantly

shifted to higher wavelength region in comparison to the P-TiO₂ nano powder, giving the order of: 1.0 wt.% Zr-Ti oxide > 1.0 wt.% Ce-Ti oxide > P-TiO₂. In term of the effect of metal oxide on the alteration of adsorption edge of TiO₂ has also reported by Zhao, *et al.*, [17]. From the obtained adsorption edge, the estimated band gap energy was calculated and the results are also listed in Table 1. The band gap decreased in the order: 1.0 wt.% Zr-Ti oxide < 1.0 wt.% Ce-Ti oxide < P-TiO₂. Modification of these electron properties of the synthesized mixed oxides is attributed to the presence of Ce and Zr.

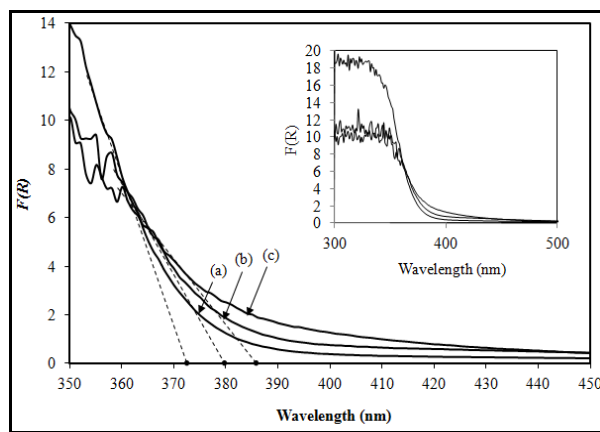


Fig. 3. A plot between Kubelka-Munk functions and wavelength of : (a) P-TiO₂, (b) 1.0 wt.% Ce-Ti oxide, and (c) 1.0 wt.% Zr-Ti oxide.

Transmission electron microscope

Transmission electron microscopy (TEM) is a versatile technique for identifying local structure of materials. Representative of a typical cluster morphology bright-field-TEM image of the synthesized P-TiO₂ nano powder is provided in Figure 4. The image seems to consist of many round shaped particle. The average particle size was estimated in the range 7.65-12.56nm. Small in size of the particle powder is also confirmed by the selected area-electron diffraction (SAED) pattern (in inset of Figure 4), showing a distinct concentric rings instead of sharp spots [22]. While the lattice fringes (in inset of Figure 4) indicates that the photocatalyst is in good crystalline nature [23]

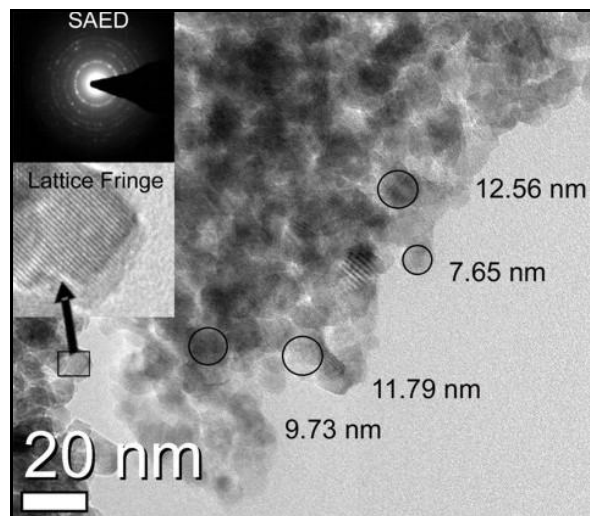


Fig. 4. Typical morphology images of synthesized P-TiO₂ nano powder (inset: SAED and enlarged lattice fringes).

CONCLUSIONS

Nanostructured powder of P-TiO₂, mixed Ce-Ti oxides, and mixed Ce-Ti oxides could be synthesized by using co-precipitation method. All synthesized nano powders are good in crystallinity and predominantly anatase phase structure. Change on the specific surface area and the absorbance edge of the synthesized mixed nano powder are attributed to the presence of CeO₂ and ZrO₂. Powder particle with nano in size and mostly spherical in shape were observed in the representative TEM images. The photocatalytic activity of these synthesized nano powder toward degradation of organic pollutant is under investigation.

REFERENCES

- [1] Carp, O., Huisman, C. L., and Reller, A., (2004), Photoinduced reactivity of titanium dioxide, *Prog. Solid State Ch.*, 32, 33-177.
- [2] Dey, G. R., (2007), Chemical reduction of CO₂ to different products during photo catalytic reaction on TiO₂ under diverse conditions: an Overview, *J. Nat. Gas Chem.*, 16, 217-226.
- [3] Kočí, K., Obalová, L., and Lacný, Z., (2008), Photocatalytic reduction of CO₂ over TiO₂ based catalysts. *Chem. Paper.*, 62, 1-9.
- [4] Linsebigler, A. L., Lu, G. and Yates, J. J. T., (1995), Photocatalysis on TiO₂ surfaces: principles, mechanisms, and selected results. *Chem. Rev.*, 95, 735-758.
- [5] Hashimoto, K., Irie, H. and Fujishima, A., (2005), TiO₂ Photocatalysis: A Historical Overview and Future Prospects, *Jpn. J. Appl. Phys.*, 44, 8269-8285.
- [6] Joshi, K. M. and Shrivastava, V. S., (2012), Removal of methylene blue dye aqueous solution using photocatalysis, *Int. J. Nano Dimens.*, 2, 241-252.
- [7] Gharbani, P., Tabatabaei, S. M., Dastmalchi, S., Ataie, S., Mosenharzandi, A. and Mehrizad, A., (2011), Adsorption of chloroform from aqueous solution by nano -TiO₂, *Int. J. Nano Dimens.*, 1, 287-296.
- [8] Amemiya, S., (2004), Titanium-Oxide Photocatalyst, *Three Bond Technical News*, 62,1-8.
- [9] Slamet, (2004), Photocatalytic reduction of CO₂ over TiO₂ and Cu-TiO₂ catalysts., Ph.D. Thesis, Chemistry University of Indonesia, Indonesia, p. 158.
- [10] Mazhdi, M. and Khani, P. H., (2012), Structural characterization of ZnO and ZnO:Mn nanoparticles prepared by reverse micelle method, *Int. J. Nano Dimens.*, 2, 233-240.
- [11] Kocí, K., Mateju, K., Obalová, L., Krejčíková, S., Lacný, Z., Plachá, D., Capek, L., Hospodková, A. and Solcová, O, (2010), Effect of silver doping on the TiO₂ for photocatalytic reduction of CO₂, *Appl. Catal. B. Environ.*, 96, 239-244.
- [12] Yoong, L. S., Chong, F. K. and Dutta, B. K., (2009), Development of copper-doped TiO₂ photocatalyst for hydrogen production under visible light, *Energy*, 34, 1652-1661.
- [13] Sasirekha, N., Basha, S. J. S. and Shanthi, K., (2006), Photocatalytic performance of Ru doped anatase mounted on silica for reduction of carbon dioxide, *Appl. Catal. B. Environ.*, 62, 169-180.
- [14] Martini, S. and Herrera, M., (2002), X-Ray diffraction and crystal size, *J. Am. Oil Chem. Soc.*, 79, 315-316.
- [15] Dhage, S. R., Gaikwad, S. P. and Ravi, V., (2004), Synthesis of nanocrystalline TiO₂ by

- tartarate gel method, *Bull. Mater. Sci.*, 27, 487–489.
- [16] Jing, L., Xin, B., Yuan, F., Xue, L., Wang, B. and Fu, H., (2006), Effects of surface oxygen vacancies on photophysical and photochemical processes of Zn-Doped TiO₂ nanoparticles and their relationships, *J. Phys. Chem. B.*, 110, 17860-17865.
- [17] Zhao, Y., Li, C., Liu, X., Gu, F., Du, H. L. and Shi, L., (2008), Zn-doped TiO₂ nanoparticles with high photocatalytic activity synthesized by hydrogen-oxygen diffusion flame. *Appl. Catal. B. Environ.*, 79, 208-215.
- [18] Antony, J., Nutting, J., Baer, D. R., Meyer, D., Sharma, A. and Qiang, Y., (2006), Size-dependent specific surface area of nanoporous film assembled by core-shell iron nanoclusters, *J. Nanomater.*, 1-4.
- [19] López, R., Gómez, R. and Llanos, M. E., (2009), Photophysical and photocatalytic properties of nanosized copper-doped titania sol-gel catalysts, *Catal. Today*, 148, 103-108.
- [20] Chen, C., Wang, Z., Ruan, S., Zou, B., Zhao, M. and Wu, F. (2008), Photocatalytic degradation of C.I. Acid Orange 52 in the presence of Zn-doped TiO₂ prepared by a stearic acid gel method, *Dyes Pigments*, 77, 204-209.
- [21] Nidhin, M., Indumathy, R., Sreeram, K. J. and Nair, B. U., (2008), Synthesis of iron oxide nanoparticles of narrow size distribution on polysaccharide templates, *Bulletin of Material Science*, 31, 93-96.
- [22] Guo, Y.-G., Hu, Y.-S. and Maier, J., (2006), Synthesis of hierarchically mesoporous anatase spheres and their application in lithium batteries, *Chemical Communication*, 2783-2785.
- [23] Karthick, S. N., Prabakar, K., Subramania, A., Hong, J.-T., Jang, J.-J. and Kim, H.-J., (2010), Formation of anatase TiO₂ nanoparticles by simple polymer gel technique and their properties, *Powder Tech.*, 205, 36-41.

Cite this article as: O. Zuas *et al.*: Anatase TiO₂ and mixed M-Anatase TiO₂ (M = CeO₂ or ZrO₂) nano powder: Synthesis and characterization.
Int. J. Nano Dimens. 4(1): 7-12, Summer 2013